



## **Free vibration analysis of FGM cylindrical shells under non-uniform internal pressure**

**I. Fakhari Golpayegani, E. Ghorbani**

*Department of Mechanical Engineering, Golpayegan University of Technology, Golpayegan, Iran*

*Received 11 Jan 2016, Revised Feb 2016, Accepted Feb 2016*

*\*Corresponding Author. E-mail: [fakhari@gut.ac.ir](mailto:fakhari@gut.ac.ir) ; Tel: (+983157241566)*

### **Abstract**

in this paper, free vibration of FGM thin cylindrical shells under non uniform linear and nonlinear internal pressure is investigated and the impact of non-uniform internal pressure on free vibrations and natural frequencies have been analyzed. The boundary conditions used in this study were two simple supported and in order to derive the equations, the theory of Sanders thin shells and Rayleigh-Ritz method is used. The effect of various parameters on natural frequencies and free vibrations of shells under internal pressure, such as linear and nonlinear pressure profile, material, thickness to radius and the ratio of length to diameter have been investigated. Additionally, the effect of internal pressure on the natural frequencies profile, in different longitudinal modes and environment has been derived. The results of this study validated by data in the literature and ABAQUS software that reflects the accuracy and can be used as a reference for future designers and researchers.

*Key words:* free vibration, natural frequency, FGM cylindrical shell, non-uniform internal pressure.

### **1. Introduction**

Cylindrical shells have many applications such as pressure vessels, structures for aerospace, aircraft, marine, etc. One of the most important parameters in the design of shells, is stability and vibration of them against the applied loads. In recent years, functionally targeted materials (FGM) for use in environments with high temperatures have been considered. In fact, these materials are composites that made of metals and ceramics which the thermal insulation capability and good toughness of ceramics and metals can be used at the same time. FGM materials are inhomogeneous that their properties change continuously and gradually from one level to another level. This operation can be applied by changing the volume ratio with a special equation. The research has been done on the field of free vibration of FGM cylindrical shells in recent years. Levy and Lam [1] investigated the effect of power factor and thickness of the shells on natural frequencies by studying the vibration of FGM shells. Haddadpor et al., [2] analyzed free vibrations of shells which made of targeted materials with heat effect and boundary conditions. Shah and mohammad [3] investigated the vibrations of FGM cylindrical shells with exponential function by Rayleigh -Ritz method and detected the impact of changing the parameters of this function on the natural frequencies. Patel et al.,[4] investigated the vibration of elliptical shells using the theory of high order and studied the impact of boundary conditions and geometrical parameters on natural frequencies. Sofia [5] studied buckling of cone shell under axial harmonic load. Tian et al.,[6] studied buckling and vibration of isotropic shells under non uniform axial and radial using Rayleigh- Ritz method. Ansari and Darvize performed dynamic analysis of FGM skins in different boundary conditions and extracted

natural frequencies in different conditions. Mohammadi and Sadegi [8] investigated the effect of pressure and temperature on free vibration and buckling of shells. In this study, effect of simultaneous pressure and temperature on free vibration is studied. Isvandzibaei [12] investigated the effect of internal uniform pressure on vibration of shells which made by graded material in different boundary conditions. They studied the effect of internal uniform pressure, number and position of rings on natural frequencies. At the listed sources, only the vibration of FGM shells under uniform internal pressure and isotropic shells under non uniform internal pressure have been investigated. However, in this article, vibration of cylindrical FGM shells with simple supported boundary conditions under non uniform internal pressure is studied using energy method. In order to derive the equations of the theory of thin shells, sanders and Rayleigh Ritz methods are used. To make simple supported conditions, the components of displacement (in longitudinal direction, circumferential and radial) considered as a combination of sine and cosine functions. The effect of various parameters such as pressure profiles, the ratio of thickness to diameter, radius and material characteristics on natural frequencies of shells investigated and results of this study verified by ABAQUS software that is an indicator of accuracy.

## 2. FGM material properties

FGM material are made from a combination of two or more materials. Most of these materials used in high temperature environments and properties of these materials define as a function of temperature according to the following equation:

$$P = P_0(P_{-1}T^{-1} + 1 + P_1T + P_2T^2 + P_3T^3) \tag{1}$$

That  $P_0, P_{-1}, P_1, P_2$  and  $P_3$  constants at temperature  $T$  in Kelvin scale and are fixed for any specific matter. The characteristics of FGM,  $P$  related to ingredient properties and volume ratio and defined as follows:

$$\tag{2}$$

$P_j$  &  $V_{fj}$  in above equation are the characteristics of materials and volume fraction  $j$ . total volume ratio of materials is equal to one.

For cylindrical shell of constant thickness  $h$  which zero surface is placed in the middle surface of the shell, the volume ratio is expressed as follows:

$$\tag{4}$$

Where  $N$  is the power law ( $0 < N \leq \infty$ ).

For shell which consist of two materials, the modulus of elasticity  $E$ , Poisson's ratio  $\nu$  and density  $\rho$  derived of the following relationships.

$$\tag{5}$$

According to this equation, in the inner surface of the shell,  $z = -h/2$ , the values of  $E = E_2, \nu = \nu_2, \rho = \rho_2$  and so for  $z = h/2, E = E_1, \nu = \nu_1, \rho = \rho_1$ . The material properties changing continuously from material 2 on inner surface of the shell to the material 1 of outer surface of the shell. Cylindrical shell made of FGM, is the membrane of non-homogeneous material which is made of homogenous and isotropic materials. For this shell

(in contrast to fiber reinforced material which the effect of shear deformation is significant because of high elastic modulus), if the thickness to radius ratio is less than 0.5, it will be possible to use theory of thin shells. In the next section, a formulation, based on Sanders's shell theory, for a functionally graded cylindrical shell is carried out.

### 3. Theory and equations

The main purpose of this section is to obtain the equations of motion for FGM thin cylindrical shell shown in figure 1, with uniform thickness  $h$ , radius  $R$ , length  $L$  and mass density  $\rho$ . The coordinates of axis of the cylinder is located in the middle surface of the membrane. Membrane displacement in the longitudinal, circumferential and radial direction ( $x, \theta, z$ ) are shown by  $u, v$  and  $w$  and velocity vectors and displacements of a point on the shell are shown by  $\bar{V}$  and  $\bar{r}$ . Velocity vector at each point of the shell is determined by following equation.

$$\bar{V} = \dot{\bar{r}} \tag{6}$$

In this equation, the displacement vector  $\bar{r}$  is as follow.

$$\tag{7}$$

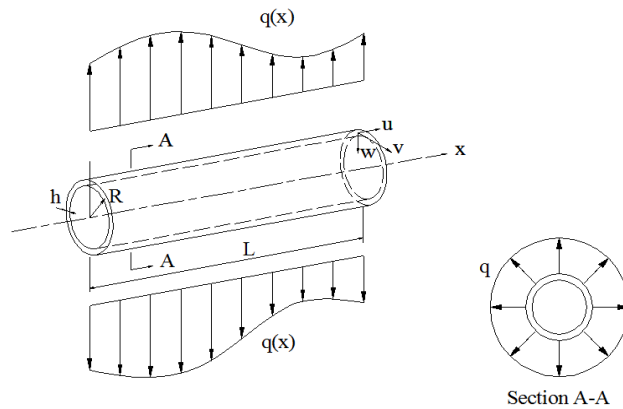


**Figure 1:** Cylindrical shell with non-uniform radial load

That  $\bar{i}, \bar{j}$  and  $\bar{k}$  are unit vectors in  $x$  and  $\theta$  and  $z$  directions, respectively.

By combining the equation (7) by equation (6), the velocity vector is obtained as follow:

$$\bar{V} = \dot{u}\bar{i} + \dot{v}\bar{j} + \dot{w}\bar{k} \tag{8}$$

In this equation  $\dot{w}$  and  $\dot{v}$  and  $\dot{u}$  are velocity components in three main directions. Kinetic energy of the shell expressed by following equation. [10]

$$T = \frac{1}{2} h \int_0^L \int_0^{2\pi} \rho \bar{V} \cdot \bar{V} R d\theta dx \tag{9}$$

In the above equation, terms of rotational inertia ignored because of thin membrane of the shell.

By putting the equation (8) in equation (9) kinetic energy of the shell can be obtained as follow:

$$T = \frac{1}{2} h \int_0^L \int_0^{2\pi} \rho [\dot{u}^2 + \dot{v}^2 + \dot{w}^2] R d\theta dx \tag{10}$$

Potential energy by pressure describes as follow:

$$U_{pr} = - \int_0^L \int_0^{2\pi} \frac{q(x)}{2} \left\{ \left[ \frac{\partial^2 w}{\partial \theta^2} + w \right] w \right\} d\theta dx \quad (11)$$

Shell tensile and flexural strain energy can be written as follow [10]

$$U_\varepsilon = \frac{1}{2} \int_0^L \int_0^{2\pi} \varepsilon^T [S] \varepsilon R d\theta dx \quad (12)$$

In this equation S is the stiffness matrix and strain vector  $\varepsilon$  as follow:

$$\varepsilon^T = \{e_1 e_2 \gamma k_1 k_2 2\tau\} \quad (13)$$

In this equation middle surface strain determined by  $e_1$   $e_2$  and  $\gamma$  and the middle surface curvature determined by  $k_1$   $k_2$  and  $\tau$ . Based on the theory of Sanders thin shells, these values are calculated as follows. [10]

$$\begin{aligned} e_1 &= \frac{\partial u}{\partial x} \\ e_2 &= -\frac{1}{R} \left( w - \frac{\partial v}{\partial \theta} \right) \\ \gamma &= \frac{\partial v}{\partial x} + \frac{1}{R} \frac{\partial u}{\partial \theta} \\ k_1 &= \frac{\partial^2 w}{\partial x^2} \\ k_2 &= -\frac{1}{R^2} \left( \frac{\partial^2 w}{\partial \phi^2} - \frac{\partial v}{\partial \phi} \right) \\ \tau &= -\frac{1}{R} \left( \frac{\partial^2 w}{\partial x \partial \phi} - \frac{3}{4} \frac{\partial v}{\partial x} \right) - \frac{1}{4R^2} \frac{\partial u}{\partial \phi} \end{aligned} \quad (14)$$

Stiffness matrix for composites is as follow:

$$[S] = \begin{bmatrix} A_{11} & A_{12} & 0 & B_{11} & B_{12} & 0 \\ A_{12} & A_{22} & 0 & B_{12} & B_{22} & 0 \\ 0 & 0 & A_{66} & 0 & 0 & B_{66} \\ B_{11} & B_{12} & 0 & D_{11} & D_{12} & 0 \\ B_{12} & B_{22} & 0 & D_{12} & D_{22} & 0 \\ 0 & 0 & B_{66} & 0 & 0 & D_{66} \end{bmatrix} \quad (15)$$

In this matrix, the tensile stiffness  $A_{ij}$ , flexural rigidity  $D_{ij}$  and torsional rigidity  $B_{ij}$  are obtained by these integral equations.

$$(A_{ij}, B_{ij}, D_{ij}) = \int_{-h/2}^{h/2} Q_{ij}(1, Z, Z^2) dz \quad (16)$$

Reduced stiffness matrix Q and the verses determines by (17)

$$\begin{aligned} Q_{11} &= Q_{22} = \frac{E}{1 - \nu^2} \\ Q_{12} &= \frac{\nu E}{1 - \nu^2} \\ Q_{66} &= \frac{E}{2(1 + \nu)} \end{aligned} \quad (17)$$

Displacement functions, u, and W considered as follow:

$$\begin{aligned} u &= A_{mn} \cos(\lambda x) \cos(n\theta + \omega t) \\ v &= B_{mn} \sin(\lambda x) \sin(n\theta + \omega t) \\ w &= C_{mn} \sin(\lambda x) \cos(n\theta + \omega t) \\ \lambda &= m\pi/L \end{aligned} \quad (18)$$

$A_{mn}$ ,  $B_{mn}$  and  $C_{mn}$  are constant mode of shape coefficient,  $m$  is the number of half – wave longitudinal wave and  $n$  is the number of half –wave circumferential waves. By substituting equation (16)and (17) in (15) stiffness matrix of shell and by substituting the equation (18) in sanders strain equations, the strain vector calculated and then according to equation (12) we can obtain potential energy of the shell. The total energy of system is as follow:

$$\Pi = T - U_{pr} - U_{\epsilon} \tag{19}$$

Using the Ritz minimizing method,

$$\frac{\partial \Pi}{\partial \Delta} = 0 \quad \Delta = A_{mn}, B_{mn}, C_{mn} \tag{20}$$

The following matrix relationship extracted:

$$\begin{bmatrix} \alpha_{11} & \alpha_{12} & \alpha_{13} \\ \alpha_{21} & \alpha_{22} & \alpha_{23} \\ \alpha_{31} & \alpha_{32} & \alpha_{33} \end{bmatrix} \begin{bmatrix} A \\ B \\ C \end{bmatrix} = \begin{bmatrix} 0 \\ 0 \\ 0 \end{bmatrix} \tag{21}$$

$\alpha_{ij}$  are the constants. For obtaining non-trivial answer of above equations, the determinant matrix must be zero.

$$\begin{vmatrix} \alpha_{11} & \alpha_{12} & \alpha_{13} \\ \alpha_{21} & \alpha_{22} & \alpha_{23} \\ \alpha_{31} & \alpha_{32} & \alpha_{33} \end{vmatrix} = 0 \tag{22}$$

After expanding the equation (22), the characteristic equations of membrane frequencies can be obtain as follow:

$$\beta_1 \omega_{mn}^6 + \beta_3 \omega_{mn}^4 + \beta_4 \omega_{mn}^3 + \beta_5 \omega_{mn}^2 + \beta_6 \omega_{mn} + \beta_1 = 0 \tag{23}$$

After solving the equation (23) using Newton-Raphson method, the natural frequencies of shell will be extracted.

#### 4. Materials

Material properties listed in this study is expressed in table 1.

**Table1:**Material properties of FGM

material	$E(N\ m^{-2}) \times 10^{11}$	$\nu$	$\rho(kg\ m^{-3}) \times 10^3$
Stainless steel	2.07788	0.317756	8.166
Zr	1.6806296	0.297996	5.7
Ni	2.05098	0.31	8.9
$Al_2O_3$	3.8	0.3	3.8

#### 5. Non - uniform internal pressure

Non-uniform internal pressure can defined as following equation and some forms of loading are shown in figure 1 and 3.

$$q(x) = P_{max} \left( 1 - \mu \left( \frac{x}{L} \right)^k \right) \tag{25}$$

In these figures, the horizontal axis represents a dimensionless number of length ( $x/L$ ) and the vertical axis represents the number of dimensionless of pressure ( $q(x)/P_{max}$ ).

Figure 2 shows the internal pressure profile line ( $k=1$ ) with different slopes  $\mu= 2,1.5,1,0.5, 0$  and figure 3 shows the non-linear pressure profile ( $\mu=1$ ) with variable power equals to  $k= 2,3,6$  and  $10$ .

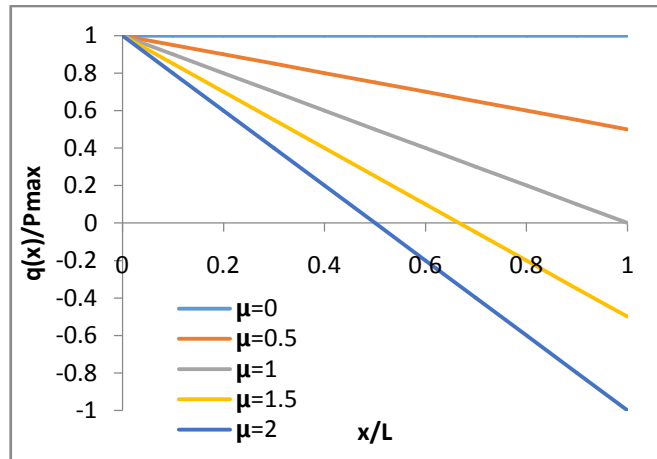


Figure 2: Linear internal pressure profile

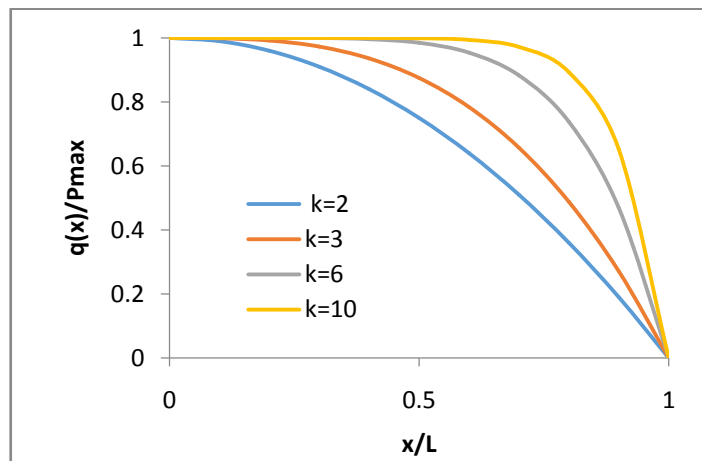


Figure 3: Non-linear internal pressure profile,  $\mu=1$

## 6. Results and discussion

To ensure the accuracy of the results obtained in this study, natural frequencies of FGM cylindrical shell compared with the results of Matsunaga in table 2, which reflects the accuracy of results. The natural frequencies for shells under uniform internal pressure [11] were compared in table 3.

**Table2:** comparison of changes of lowest natural frequencies (Hz) with reference [9], ( $m=1$   $L/R=20$ , inner surface of nickel and outer surface of steel)

h/R	h/R	n	N=1	N=2	N=5	N=15
Ref. [9]	0.001	3	2.7235	2.7015	2.6788	2.6635
Present		3	2.7236	2.7014	2.6789	2.6635
Ref. [9]	0.005	2	5.3627	5.3192	5.2747	5.2449
Present		2	5.3627	5.3192	5.2746	5.2449
Ref. [9]	0.010	2	7.7286	7.6664	7.6024	7.5581
Present		2	7.7286	7.6663	7.6024	7.5582
Ref. [9]	0.030	1	13.2119	13.1042	12.9984	12.9333
Present		1	13.2120	13.1042	12.9985	12.9334

Figure 4 shows the effect of FGM membrane ingredients on the natural frequencies. As it is clear from the figure, the highest natural frequency is respectively to alumina shell- stainless steel, zirconia-alumina, zirconium-stainless steel and nickel- stainless steel. Higher natural frequency of alumina-stainless steel in comparison of other components is because of high elastic modulus and low density of alumina.

**Table 3:** comparison of shell natural frequency under uniform internal pressure of 1 bar with reference [11] and software, ( $L/R=20$ ,  $m=1$ ,  $h/R=0.002$ , inner surface of nickel and outer surface of steel)

n	1	2	3	4	5	6	7	8	9	10
Ref. [11]	13.21	19.37	32.94	46.3	59.59	72.97	86.56	100.46	114.72	129.41
ABAQUS	13.1415	19.3525	32.9387	46.3012	59.5954	72.9774	86.5769	100.4905	114.7824	129.5138
Present	13.2111	19.4714	33.1077	46.5355	59.8794	73.8183	86.9706	100.9215	115.2381	129.9768

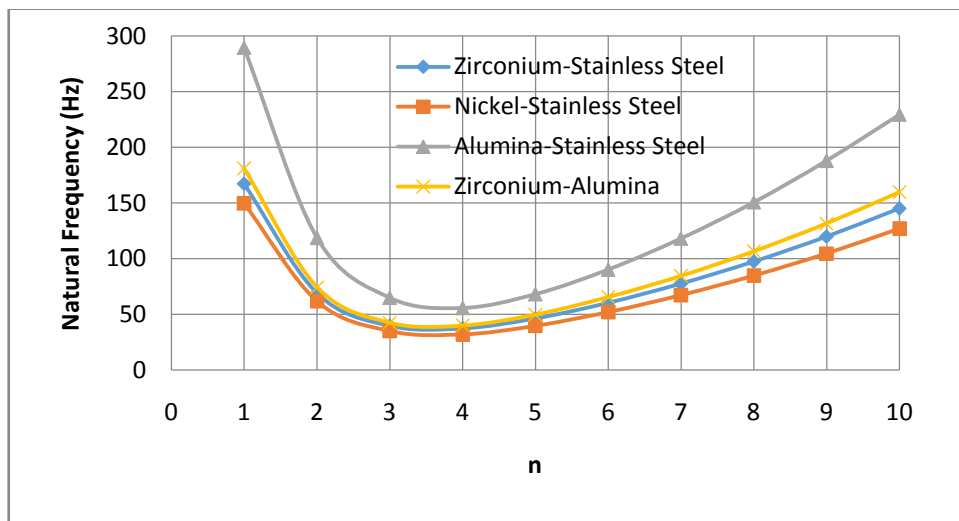


**Figure4:**The natural frequencies of different combinations of FGM cylindrical shell in number of circumferential wave (n).

In table 4, the natural frequencies of FGM cylindrical shell under pressure up to 100 kPa, with the ratio of length to diameter 5 and ratio of thickness to radius of 0.005 is shown with inner surface of zirconium and outer surface of nickel for different power functions of uniform and non-uniform internal pressures.

As is clear from the table increasing the power factor volume (N) natural frequency is reduced. Also for all loading conditions, the first natural frequency decreased and after reaching the base frequency rises again. Circumferential wave number (n) which the base frequency occurs at that number, varied by changing the load profile and by more closing of uniform pressure to the base frequency, the base frequency happens in lower circumferential number. With increasing pressure function coefficient ( $\mu$ ) natural frequency decreases and with increasing power function of pressure (k), natural frequency increases. Also in this table, in the case of  $N=1$  analytical results (row 1) compared to the software results (row 2) and showing high accuracy of results. It is clear from the numbers of table that changing in loading profile in  $n=1$ , has no effect on the natural frequency. Tables 5 and 6 show the natural frequencies under maximum pressure of 50 kPa with inner surface of alumina and outer surface of stainless steel. As it is known, by increasing the ratio of thickness to radius in both linear and non-linear loading, the natural frequency increases and by increasing the ratio of length to radius in both linear and non-linear loading, natural frequency decreases. In the case of linear internal pressure, by increasing the  $\mu$ , the base natural frequency decreases and increases in non-linear mode. The main reason for this case is

that by in linear mode, by increasing  $\mu$ , non-uniform pressure distances with the uniform pressure, but in the case of non-linear pressure, with increasing of  $K$  it is approaching to the uniform pressure.

**Table 4:** Comparison of natural frequencies of membrane (Hz) under  $P_{max}=100kPa$  ( $L/R=5$ ,  $h/R=0.005$ ,  $m=1$ , inner surface of nickel and outer surface of zirconium)

N	n	Linear internal pressure					Non-linear internal pressure				
		$\mu=0,k=1$	$\mu=0.5,k=1$	$\mu=1,k=1$	$\mu=1.5,k=1$	$\mu=2,k=1$	$\mu=1,k=2$	$\mu=1,k=3$	$\mu=1,k=6$	$\mu=1,k=10$	
N=0.5	1	160.49720	160.49720	160.49720	160.49720	160.49720	160.49720	160.49720	160.49720	160.49720	
	2	66.802301	66.471948	66.139941	65.806257	65.470869	66.428652	66.572537	66.72822	66.77693	
	3	<b>41.213895</b>	39.554763	37.822913	36.007853	34.096298	39.332759	40.066348	<b>40.847</b>	<b>41.08857</b>	
	4	42.026872	<b>38.762572</b>	<b>35.196807</b>	<b>31.226474</b>	<b>26.671507</b>	<b>38.315415</b>	<b>39.783145</b>	41.31594	41.78468	
	5	52.634305	48.360940	43.671389	38.413526	32.311097	47.774215	49.698774	51.70496	52.31778	
N=1	1	157.11492	157.11492	157.11492	157.11492	157.11492	157.11492	157.11492	157.11492	157.11492	
		157.15	157.15	157.15	157.15	157.15	157.15	157.15	157.15	157.15	
	2	65.358646	65.045703	64.731244	64.415248	64.097690	65.004693	65.140986	65.28847	65.33461	
		65.457	65.152	64.847	64.539	64.23	65.117	65.252	65.396	65.44	
	3	<b>40.127341</b>	38.548502	36.902167	35.178861	33.366659	38.337358	39.035168	<b>39.77808</b>	<b>40.00803</b>	
		<b>40.337</b>	38.772	37.138	35.424	33.618	38.563	39.258	<b>39.998</b>	<b>40.225</b>	
	4	40.703410	<b>37.580698</b>	<b>34.173812</b>	<b>30.387321</b>	<b>26.056254</b>	<b>37.153200</b>	<b>38.556653</b>	40.02305	40.47161	
		40.928	<b>37.807</b>	<b>34.359</b>	<b>30.468</b>	<b>25.94</b>	<b>37.321</b>	<b>38.746</b>	40.246	40.701	
	5	50.931660	46.839792	42.354427	37.334007	31.523926	46.278297	48.120393	50.04148	50.62846	
		51.11	46.937	42.40	36.483	29.5	46.065	48.037	50.165	50.802	
N=5	1	151.48968	151.48968	151.48968	151.48968	151.48968	151.48968	151.48968	151.48968	151.48968	
	2	62.961971	62.678614	62.393968	62.108016	61.820738	62.641487	62.764880	62.89842	62.94021	
	3	<b>38.317029</b>	36.875772	35.375838	33.809418	32.166801	36.683229	37.319751	37.99798	<b>38.20803</b>	
	4	38.466785	<b>35.586704</b>	<b>32.452008</b>	<b>28.980192</b>	<b>25.031373</b>	<b>35.192892</b>	<b>36.486202</b>	<b>37.83881</b>	38.25281	
	5	48.027346	44.244572	40.106580	35.489333	30.173616	43.726025	45.427732	47.20387	47.74683	
N=20	1	149.77581	149.77581	149.77581	149.77581	149.77581	149.77581	149.77581	149.77581	149.77581	
	2	62.235967	61.961824	61.686460	61.409860	61.132004	61.925906	62.0452821	62.17448	62.21491	
	3	<b>37.789268</b>	36.392076	34.939048	33.492904	31.834624	36.205491	36.822381	37.47989	37.68357	
	4	37.854371	<b>35.056745</b>	<b>32.015570</b>	<b>28.653404</b>	<b>24.840243</b>	<b>34.674447</b>	<b>35.930173</b>	<b>37.24413</b>	<b>37.64642</b>	
	5	47.279968	43.607056	39.594882	35.127389	30.001858	43.103921	44.755385	46.48005	47.00746	

Figures 5 and 6 show the decrease in natural frequencies when the loading is linear and  $\mu$  coefficient increases from 0 to 10. In this case, the ratio of length to radius of shell equals to 5 and the ratio of thickness to radius equals to 0.005. The greatest reduction occurs in the smallest natural frequency ( $m=1$ ) and highest number of circumferential wave ( $n$ ). In figure 5 the power-law exponent equals to 1 and in figure 6 the power-law exponent equals to 20. By comparing these figures, we find that the Percent reduction in natural frequency have inversely relation with  $N$ .



**Table 5:** Comparison of natural frequencies of membrane (Hz) under  $\rho P_{max}=kPa$  (L/R=5, N=5,m=1, inner surface of alumina and outer surface of stainless steel)50

		Linear internal pressure					Non-linear internal pressure		
h/R		$\mu=0, k=1$	$\mu=0.5, k=1$	$\mu=1, k=1$	$\mu=1.5, k=1$	$\mu=2, k=1$	$\mu=1, k=2$	$\mu=1, k=6$	$\mu=1, k=10$
Present	0.003	52,19345	48,94587	45,4669	41,69871	36,400051	48,50538	51,48165	51,950699
Abaqus		52,394	49,154	45,662	41,855	35,435	48,688	51,686	52,157
Present	0.005	52,904160	51,007418	49,0373	46,98477	44,838312	50,75429	52,48398	52,760589
Abaqus		53,339	51,462	49,498	47,448	45,3	51,201	52,926	53,2
Present	0.007	58,93072	57,723788	56,4910	55,23085	53,941190	57,56418	58,66171	58,838701
Abaqus		59,759	58,564	57,343	56,092	54,811	58,405	59,495	59,669
Present	0.01	66,099568	65,719619	65,3374	64,95305	64,656355	65,66980	66,01439	66,070401
Abaqus		67,1	66,727	66,352	65,975	65,959	66,68	67,019	67,074
Present	0.03	112,63826	112,56408	112,489	112,4155	112,34124	112,554	112,6216	112,63265
Abaqus		115,33	115,26	115,19	115,12	115,05	115,25	115,39	115,33
Present	0.05	126,94236	126,92938	126,916	126,90344	126,89046	126,9276	126,9394	126,94136
Abaqus		132,72	132,71	132,7	132,68	132,67	132,71	132,72	132,72

**Table 6-** Comparison of natural base frequencies of membrane (Hz) under  $\rho P_{max}=50kPa$  (h/R=0.005, N=5,m=1, inner surface of alumina and outer surface of stainless steel)

		Linear internal pressure					Non-linear internal pressure		
L/R		$\mu=0, k=1$	$\mu=0.5, k=1$	$\mu=1, k=1$	$\mu=1.5, k=1$	$\mu=2, k=1$	$\mu=1, k=2$	$\mu=1, k=6$	$\mu=1, k=10$
Present	1	205,86518	200,92653	195,16256	189,22309	183,091	200,18266	204,8586	205,5209
Abaqus		212,42	207,59	201,97	196,16	190,16	206,93	211,61	212,22
Present	5	52,193455	48,945879	45,466922	41,698711	36,40005	48,505387	51,48165	51,950699
Abaqus		52,394	49,154	45,662	41,855	35,435	48,688	51,686	52,157
Present	7	40,085350	37,940988	35,667934	30,737227	24,81942	37,651717	39,61368	39,924389
Abaqus		40,169	38,028	35,607	30,364	23,864	37,731	39,7	40,011
Present	10	31,112407	28,291410	25,15602	21,569585	17,25302	27,901665	30,50133	30,904422
Abaqus		31,148	28,311	25,108	21,374	14,305	27,855	30,524	30,939
Present	13	23,633459	22,423960	21,145388	18,163880	12,73717	22,261035	23,36717	23,542571
Abaqus		23,64	22,437	21,156	17,354	10,539	22,268	23,375	23,55
Present	15	20,465555	19,054526	17,530284	15,860220	11,4009	18,862320	20,157139	20,360421
Abaqus		20,468	19,061	17,526	15,759	12,615	18,855	20,159	20,364

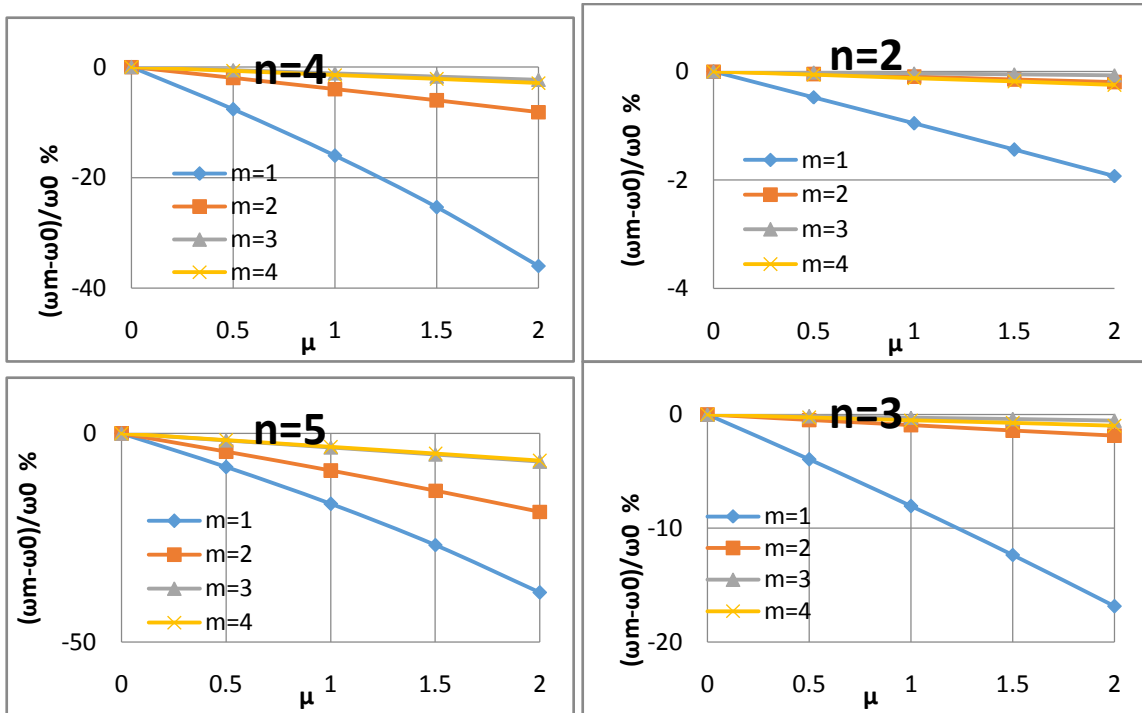


Figure 5: dimensionless natural frequencies in  $\mu \cdot k=1$ ,  $L/R=5$ ,  $h/R=0.005$ ,  $N=1$ ,  $P=100$  kpa ( $\omega_m=\omega_0$  when  $\mu=0$ )

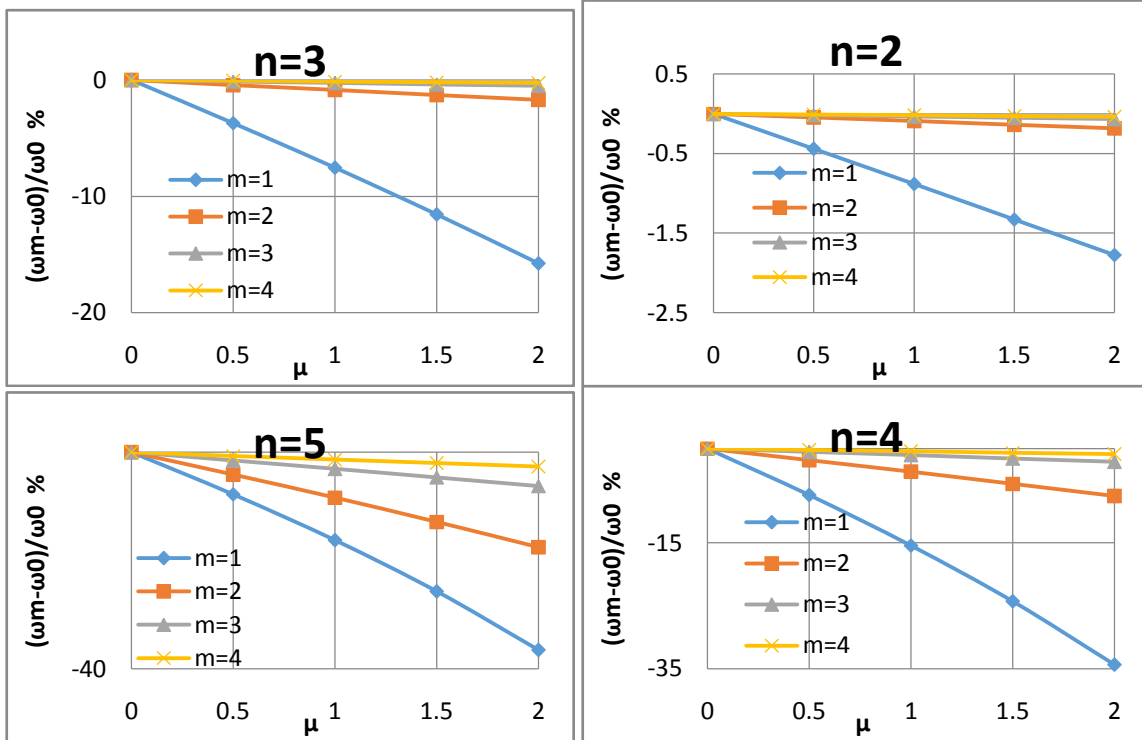


Figure 6: dimensionless natural frequencies in  $\mu \cdot k=1$ ,  $L/R=5$ ,  $h/R=0.005$ ,  $N=20$ ,  $P=100$  kpa ( $\omega_m=\omega_0$  when  $\mu=0$ )

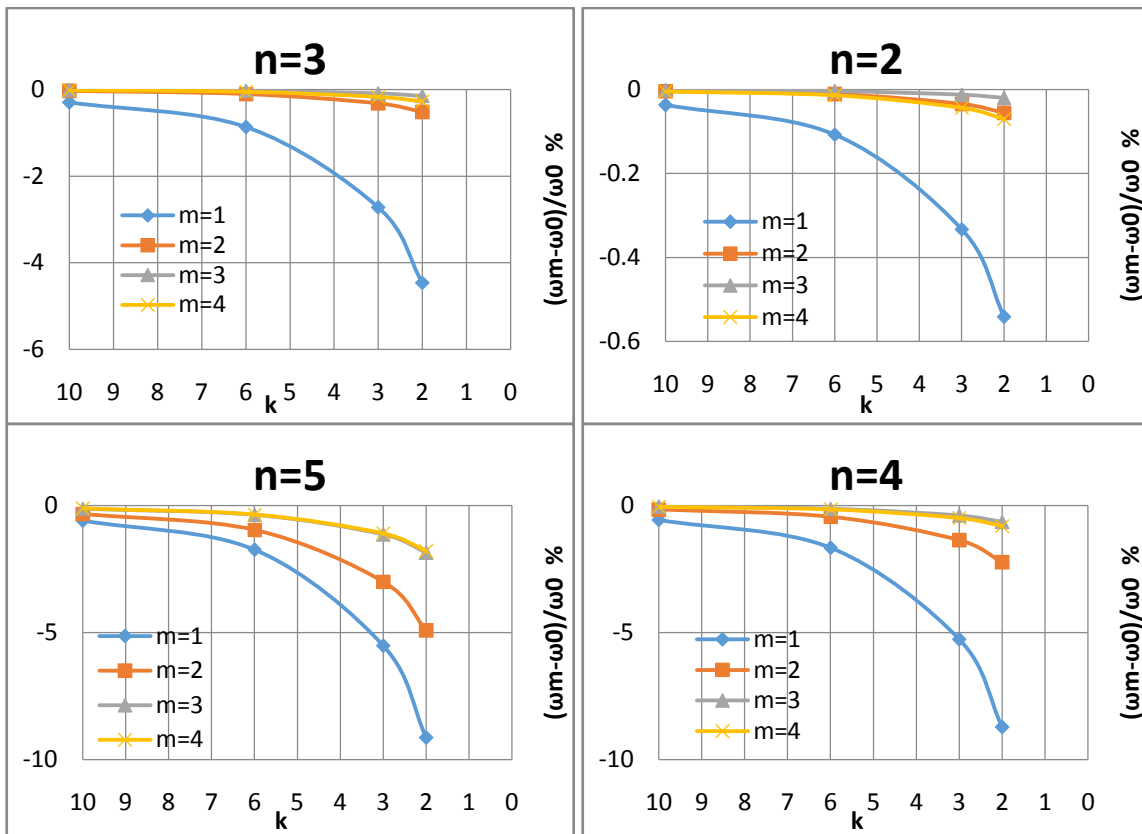


Figure 7: dimensionless natural frequencies in  $k, \mu=1, L/R=5, h/R=0.005, N=1, P=100$  kpa ( $\omega_m=\omega_0$  when  $k=0$ )

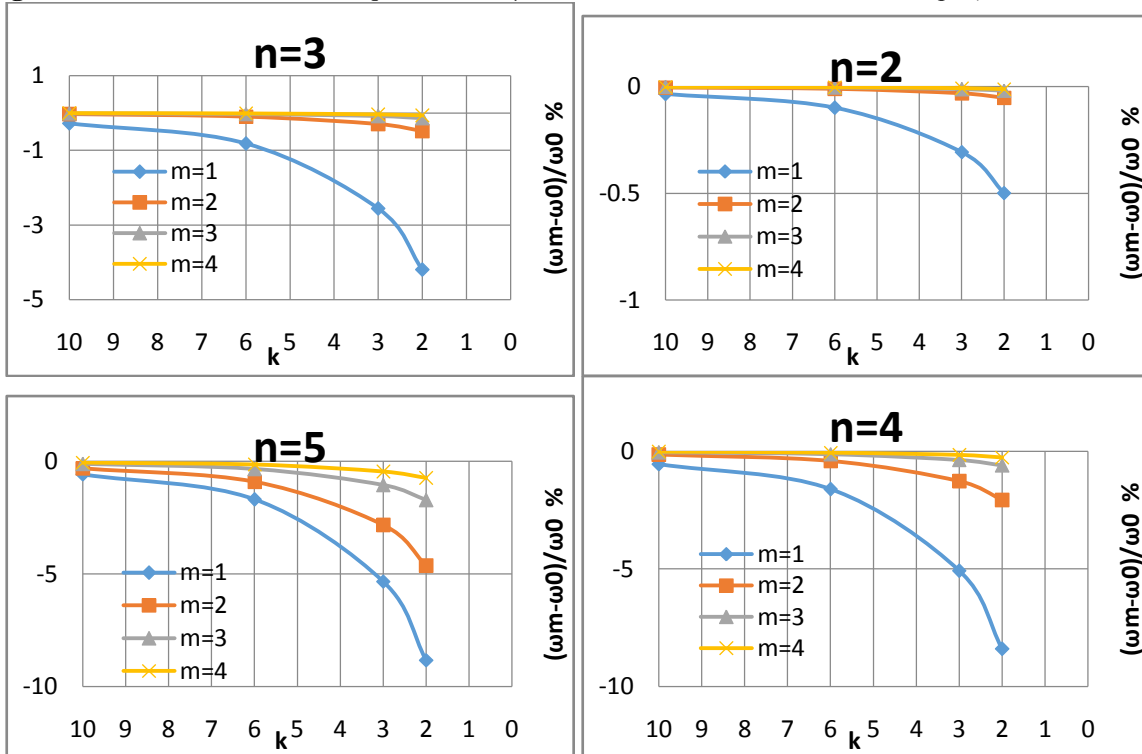


Figure 8: dimensionless natural frequencies in  $k, \mu=1, L/R=5, h/R=0.005, N=20, P=100$  kpa ( $\omega_m=\omega_0$  when  $k=0$ )

In figure 7 and 8 power function of internal pressure changes between 2 and 10 when  $\mu$  equals to 1. In this case the ratio of length to radius equals to 5 and the ratio of thickness to radius equals to 0.005. The greatest reduction occurs in the smallest natural frequency ( $m=1$ ) and the highest number of circumferential wave number ( $n$ ). By increasing  $n$ , the distance between the charts increases for  $m$  numbers greater than 1. Also the reduction percentage in lower numbers of pressure function coefficient ( $k$ ) is more. Figure 7 shows the reduction of the natural frequency by a volume factor of 1 and figure 8 shows the reduction of natural frequency by a volume factor of 20. By comparing these figures we can see that with increasing  $N$ , reduction percent of natural frequency decreases.

## Conclusion

In this study free vibration of cylindrical shells with simply supported boundary conditions under linear and non-linear internal pressure was studied. To derive the equations of motion, the Sanders's thin shells theory and Rayleigh-Ritz method used and the effect of various parameters such as internal pressure profile, the ratio of thickness to radius, the ratio of length to radius and material on natural frequencies was investigated. In all cases the natural frequency dropped at first stage and after reaching the fundamental frequency rises again. Circumferential wave number ( $n$ ) which is the fundamental frequency occurs at that number, varied by changing the load profile and by more closing of load profile to the uniform pressure, the base frequency happens in lower circumferential number. With increasing the pressure load coefficient ( $\mu$ ) the natural frequency decreases and increases when power of pressure function ( $k$ ) increases. In the case of linear internal pressure, by increasing the  $\mu$  the fundamental natural frequency decreases and increases in non-linear mode. By increasing the  $\mu$  coefficient and decreasing  $k$  power, the greatest reduction occurs in the smallest natural frequency ( $m=1$ ) and highest number of circumferential wave ( $n$ ). With increasing  $N$ , reduction percent of natural frequency decreases in nonlinear and linear pressure load.

## References

1. Loy C.T., Lam K.Y., and Reddy J.N., *International Journal of Mechanical Sciences* 41 (1999) 309-324.
2. Haddadpour H., Mahmoudkhani S., and Navazi H.M., *Thin-Walled Structures* 45 (2007) 591-599.
3. Shah A.G., Mahmood T., and Naeem M.N., *Appl. Math. Mech. -Engl. Ed.* 30(5) (2009) 607-615.
4. Patel B.P., Gupta S.S., Loknath M.S., and Kadu C.P., *Composite Structures* 69 (2005) 259-270.
5. Sofiyev A.H., *Journal of Sound and Vibration* 305 (2007) 808-826.
6. Tian J., Wang C.M., Swaddiwudhipong, S., *Thin-Walled Structures* 35 (1999) 1-24.
7. Ansari R. and Darvizeh, M., *Composite Structures* 85(4) (2008) 284-292.
8. Mohammadi F., Sedaghati R., *Journal of Sandwich Structures and Materials* 14(2) (2011) 157-180.
9. Matsunaga H., *Composite Structures* 88(4) (2009) 519-531.
10. Zhao X., Liew K.M., and Ng T.Y., *International Journal of Solids and Structures* 39 (2002) 529-545.
11. Azimi P., Mehrabani M.M. and Jafari A.A., *Magazine of mechanic-aerospace* 7 (2011) 81-90.
12. Isvandzibaei M. R., Jamaluddin H., Raja Hamzah R. I., *Acta-mech* 225 (2014) 2085-2109.

(2016) ; <http://www.jmaterenvirosnci.com>